1-17-1997

Modeling Of The Underwater Light Field And Its Effect On Temperature, Stability, And Momentum

Charles R. Bostater

Ted McNally

Wei-ming Ma

PROCEEDINGS OF SPIE

SPIEDigitalLibrary.org/conference-proceedings-of-spie

Modeling of the underwater light field and its effect on temperature, stability, and momentum

Charles R. Bostater
Ted McNally
Wei-ming Ma

SPIE.

Modeling of the underwater light field and its effect on temperature, stability, and momentum

Charles Bostater, Ted McNally, and Wei-ming Ma

Marine and Environmental Optics Laboratory, Center for Remote Sensing
Marine and Environmental Systems Division
Florida Institute of Technology
150 West University Blvd.
Melbourne, FL 32937

ABSTRACT

A model of the subsurface irradiance distribution that is based on the two-flow equations and allows for variations of the concentrations of various water quality constituents (chlorophyll-a, dissolved organic matter, and suspended matter) with depth has been described by Bostater, Ma, and McNally[1]. This model allows output of the irradiance spectra at various depths. By combining the two-flow model with the hydrodynamic model of Blumberg and Mellor[2], the effect of the absorption of irradiance as a function of wavelength and depth on water temperature, density, turbulent kinetic energy (TKE), pressure, and the resulting circulation in an idealized ocean basin is studied. The two-flow model is set up to allow variation of the water quality parameters to occur in three layers, any number of layers, or to be constant with depth and thus affect the absorption of the sun's energy. Three simulations were run using (a) clear water coefficients, (b) a vertical distribution of chlorophyll, and (c) a vertical distribution of suspended sediments. For comparison, coefficients and attenuation for various water types included in the Princeton Ocean Model were used for comparison.

1. INTRODUCTION

One of the most persistent features of the world's ocean and coastal waters is the existence of a well mixed, warmer, surface layer distinct from the colder deeper water masses and bounded by a region know as the thermocline[3]. At mid-latitudes, ocean waters tend to exhibit two different thermoclines: a permanent thermocline between 500 and 1000 m, and a seasonal thermocline in the summer very near the surface[3]. It is in this homogeneous region that most of the sun's radiant energy is absorbed, and any physical (diffusion, advection, turbulent energy production or dissipation), biological (photosynthesis, grazing), or chemical (photolysis, solubilization) processes in this area are affected by the absorption of the downwelling irradiance. As numerical ocean models have advanced from simple, vertically averaged, barotropic models driven primarily by wind and tidal forcings to complex, three dimensional, baroclinic models (such as the Princeton Ocean Model[2] with its second order turbulent closure scheme), accurate parameterization of the downwelling solar flux needs to be introduced and evaluated. As a first approximation, many models[2] use a simple exponential decay of the solar flux with depth:

$$E_d^w(z) = E_d^w(0)e^{\alpha z}\ , \tag{1}$$

where $E^w_d(z)$ (units Wm^{-2}) is the downwelling irradiance at depth z, $E^w_d(0)$ (units Wm^{-2}) is the downwelling irradiance just below the water surface, α is an attenuation coefficient for the downwelling irradiance (units m^{-1}), and z is depth (units m). Equation 1 is a common expression for the decay of downwelling irradiance with depth. Other models have simulated the light field as a function of wavelength (λ). In either case, sacrifices must be made. For a simple exponential decay model, the differential penetration of the short-wave radiation versus the longer wave radiation in clear oceanic waters is not explicitly accounted for.

In this paper we describe the application of a computationally efficient analytical solution to the two-flow equations to quantify the underwater light field. The model [1,4,5,6] utilizes unique boundary conditions to solve the well know two-flow irradiance equations[7,8,9,10]. The model (described in detail in the next section) is simple, yet powerful. It allows for the concentration of water quality parameters (chlorophyll-a, seston, dissolved organic carbon) to be varied within any number of homogeneous layers. The inherent optical properties (absorption and backscatter) necessary as input into the two-flow model can then be calculated as described in Section 2.1. The solution solves for the downwelling irradiance through each

layer until it impinges upon the bottom or is completely attenuated. The upwelling irradiance is also calculated for each layer. By varying the concentrations of water quality parameters, and thus varying the inherent optical properties, with depth, the layered Case I [1,4,5,6] two-flow irradiance model allows for realistic simulations of the underwater light field that are computationally less complex than radiance models, but more detailed than simple exponential decay models.

The model is easily incorporated as a subroutine into the existing Princeton Ocean Model, and is capable of producing realistic downwelling irradiance profiles at wavelength resolutions of 1 nm as well as useful reflectance signatures[1]. Section 2 is a description of the overall model, while Section 3 details the two-flow equations and their solutions which have been previously reported[1,4,5,6]. In Section 4 we describe a number of test cases to which the model was applied, and in Section 5 we draw conclusions and directions for further study.

2. OVERVIEW OF THE MODEL

In order to accurately model the underwater light field, it is first necessary to know $E^a_d(0)$, the downwelling irradiance at the water's surface. In order to find the downwelling irradiance incident on the water surface, the model uses published values of the solar constant as a function of wavelength (the solar irradiance incident on the edge of the earth's atmosphere) from Valley[11] in the range from 300 to 1100 nm. This radiation incident on the edge of the atmosphere is scattered and attenuated in the earth's atmosphere before it reaches the water's surface. Extinction coefficients from Elterman[12] are used to calculate the irradiance incident on the earth's surface using a simple exponential decay relationship similar to Equation 1 where z=12.85 km (the distance from the earth's surface to the edge of the atmosphere where Valley's measurements were made).

Once the direct sunlight at the earth's surface has been calculated, the amount of diffuse irradiance can be calculated as a simple proportion of the direct flux[13]. Some of the radiation incident on the water's surface is transmitted into the water column, and some is reflected back into the atmosphere. The model uses the Fresnel reflectance equation given in Priesendorfer[9] to calculate the amount of the direct irradiance reflected and from that, the amount transmitted into the water column is estimated. A second reflectance equation (also from Priesendorfer[9]) is used to find the amount of diffuse irradiance reflected and transmitted. Once the direct and indirect irradiance just below the water's surface has been calculated, all of the direct irradiance is assumed to be converted to diffuse irradiance (Case I model), and the calculation of upwelling and downwelling irradiance proceeds as described in Section 3 below.

Irradiance absorbed beneath the surface is converted to a temperature flux according to:

$$R(i) = \frac{E_d^w(i)}{c_p \rho} \tag{2}$$

where:

$R(i)$ is the temperature flux (mKs^{-1}) at i,
$E_d^w(i)$ is the irradiance (Wm^{-2}) at absorbed within layer i,
c_p is the specific heat of water
taken to be constant 3900 $Jkg^{-1}K^{-1}$, and
ρ is the density (mgm^{-3}) of the water also taken
to be constant 1025 kgm^{-3}.

This temperature flux enters into the equation for potential temperature, and potential temperature is used in a truncated equation of state to calculate density. The density is then used in the momentum equations to calculate velocities. It is through this procedure that changes in the underwater light field cause changes in the other physical characteristics of the ocean.

2.1 The absorption and backscatter coefficients

The absorption and backscatter coefficients in each layer are calculated using Bukata's[14] algorithm where the total absorption coefficient (a) as a function of wavelength is taken to be the sum of the absorption coefficients due to chlorophyll-a, seston, and dissolved organic carbon:

$$a = a_{water} + a_{ss}c_{ss} + a_{doc}c_{doc} + a_{chl}c_{chl}, \tag{3}$$

where a_{water}, a_{doc}, a_{chl}, and a_{ss} are the specific absorption coefficients for water, dissolved organic carbon, chlorophyll-a, and seston, respectively. Each of these are a function of wavelength and have units of length^2/mass. Value of the specific absorption coefficients are given in Bukata[14], Smith and Baker[15] (for pure sea water), and Bostater and Gimond[16,17]. The symbols c_{ss}, c_{doc}, and c_{chl} are the concentrations of seston (mgL^{-1}), dissolved organic carbon (mgL^{-1}), and chlorophyll-a (μgL^{-1}). A similar expression for the total backscatter coefficient (b) is also given[14]:

$$b = b_{water} + b_{ss}c_{ss} + b_{chl}c_{chl}, \tag{4}$$

where b_{water}, b_{ss}, and b_{chl} are the specific backscatter coefficients for water, seston, and chlorophyll-a that have the same units as the specific absorption coefficients. In the model, the concentrations of chlorophyll-a, seston, and dissolved organic carbon are input for each layer, and the total absorption and backscatter coefficients calculated from the concentration.

3. THE LAYERED TWO-FLOW EQUATIONS

The analytical solution to the two-flow equations used in the layered model are given in Bostater, et al. [1,4,5,6], and their derivation will not be repeated here except to give the final equations, in layered form, for the Case I model below the surface:

$$E_d^w(i) = \frac{E_d^w(i-1)}{2}X + \frac{-kE_d^w(i-1)}{2\Psi}Y, \tag{5}$$

$$E_u^w(i) = \frac{E_u^w(i+1)}{2}V - \frac{(a_{i+1}+b_{i+1})E_u^w(i+1) - b_{i+1}E_d^w(i+1)}{2\Psi}W, \tag{6}$$

where

$$X = e^{\Psi h} + e^{-\Psi h}, \tag{7}$$

$$Y = e^{\Psi h} - e^{-\Psi h}, \tag{8}$$

$$V = e^{\Psi(z-h)} + e^{-\Psi(z-h)}, \tag{9}$$

$$W = e^{\Psi(z-h)} - e^{-\Psi(z-h)}, \tag{10}$$

and

$$\Psi = \sqrt{(a_i)^2 + 2a_i b_i}\ . \tag{11}$$

In the surface layer, k, the attenuation coefficient, is calculated using a formulation from Gordon[18]:

$$k = \frac{a+b}{\mu} \tag{12}$$

where:
a is the absorption coefficient (m^{-1}),
b is the backscatter coefficient (m^{-1}), and
μ is the cosine of the zenith angle of the sun.

In the second layer:

$$k = -\frac{1}{E_d(0.5)} \frac{E_d(1) - E_d(0.5)}{z(1) - z(0.5)}, \tag{13}$$

and in the third and deeper layers:

$$k = -\frac{1}{E_d(i-2)} \frac{E_d(i-2) - E_d(i-1)}{z(i-2) - z(i-1)} \tag{14}$$

4. MODEL TEST CASES

The Princeton Ocean Model[2] was set up to loosely model the North Atlantic Ocean (from 20N to 60N and 70W to 30W) on a 20x20 ($\Delta x = \Delta y = 2$ degree or 2.22×10^5 m) grid with 24 vertical layers and a constant bottom depth of 2000 m. The internal time step was one hour, and the external time step two minutes. The vertical layers (σ coordinates) were set to give greatest vertical resolution in the upper portion of the 2000 m basin. A constant (in time) cosine wind stress was applied to the basin in all model runs. The vertical temperature profile for all model runs was initialized to 10 degrees Celsius throughout the water column. The layered two-flow model described above was converted into a subroutine in the Princeton model to calculate the change in irradiance over each σ level. Each simulation was run for 30 days. The model reaches steady state after about 20 days, with velocities varying by less that 10^{-3} ms^{-1} from time step to time step.

Each day in the simulation was assumed to consist of two 12 hour periods. During the first 12 hours, no flux of solar energy was assumed at the surface of the ocean (night). During the second 12 hours of each day, the zenith angle of the sun was varied linearly from 90 degrees up to its maximum of 20 degrees after 6 hours, and then back down to 90 degrees over the next 6 hours to roughly simulate summer conditions. The zenith angle, and solar flux, was assumed to be constant in the model domain. The Princeton model was run with (a) the new "two-flow" subroutine for clear water, once with a vertical distribution of chlorophyll (Figure 2), once with a vertical distribution of suspended sediments (constant 10 mg/L throughout the water column), and also (b) with the standard exponential attenuation coefficients derived from Jerlov's data for Type I (very clear) and Type IV (higher chlorophyll concentration) waters to allow for a comparison between the two models.

5. RESULTS AND CONCLUSIONS

Figures 2-7 show vertical temperature profiles from the Princeton model. On a large vertical scale (2000 m), there is little significant difference between the temperature profiles (as observed in Figures 2,4, and 6), but at or near the surface one can clearly observe a difference of up to 6 degrees Celsius between the temperature calculated using simple exponential attenuation and the temperature calculated using the more realistic two-flow equations for irradiance transfer. Additionally, the two flow model shows a more significant increase in surface temperatures as the water becomes more turbid (Figures 3 and 5). This last point is very significant from an environmental point of view as coastal waters (important for recreational and economic reasons) tend to be more turbid than open ocean water.

Figure 8 show static stability (E) calculated from the model output for clear, turbid, and productive water. Static stability was calculated using the simple relation[3]:

$$E = -\frac{1}{\rho}\frac{\delta\rho}{\delta z}, \tag{15}$$

where ρ is the density of the layer and $\frac{\delta\rho}{\delta z}$ is the change in density over the layer. All three cases using the two-flow attenuation are more stable than the case for exponential attenuation for clear water. Figures 9 and 10 are zonal and meridional velocities after 30 days. Figure 11 show the vertical velocity as a function of depth for the different model runs. Note that the clear water (dashed line) using two-flow attenuation shows sinking (negative vertical velocities) near the surface with rising water below thirty meters. This would seem to indicate that the clear water is allowing more energy to reach greater depths causing greater instability. Figure 8 supports this conclusion in that the clearer water (dashed line) is also less stable at those depths.

The layered two-flow irradiance model described here produces significantly higher temperatures in the upper few meters of the ocean when compared to the exponential attenuation model. Both methods of parameterizing the underwater irradiance are capable of reproducing the seasonal and permanent thermocline. The application of a layered two-flow model allows for a greater diversity of water types that can be simulated by allowing the concentrations of three water quality parameters to vary as a function of depth. Further enhancements to the irradiance model are in progress. These include using the Case II two-flow equations (that explicitly evaluate the specular light) to form the layered model and the investigation of cloud effects.

6. ACKNOWLEDGEMENTS

Model simulations were performed on an Indigo^2 workstation. Indirect support has been provided by Sid Mair, Silicon Graphics Inc., and K.B. Science and Engineering. Dr. William Naught, Ken Poimbeouf, NASA, Kennedy Space Center, are acknowledged for supporting this research. Dr. R. Sullivan, Florida Tech, is thanked for his support in the development of the Marine and Environmental Optics Lab, Remote Sensing Center at Florida Tech.

7. REFERENCES

1. C. Bostater, W. Ma, and T. McNally, "Advancement of an optical remote sensing model to simulate the underwater light field," in press: *Proc. European Optical Society and SPIE - The International Society for Optical Engineering (EUROPTO), The European Symposium on Satellite Remote Sensing III*, Taormina, Italy, 23-27 September, 1996, 9 pp.

2. A. Blumberg and G. Mellor, A description of a three-dimensional coastal ocean model, in *Three Dimensional Shelf Models, Coastal Estuarine Sci.*, vol. 5, edited by N. Heaps, pp. 1-16, AGU, Washington, D. C., 1987.

3. G. Pickard and W. Emery, *Descriptive Physical Oceanography*,5th ed., Pergamon Press, Tarrytown, NY, 1990, 320 pp.

4. C. Bostater, W. Ma, and A. Lamb, "Simulating radiative transfer in aquatic systems and contrasting results from ambient environmental spectroscopy. estuarine and near coastal waters," In: *Proc. 2nd Intl. Symp. on Spectral Sensing Research*, San Diego, CA, USACOE, July, 1994, pp. 673-682.

5. C. Bostater, W. Ma, T. McNally, M. Gimond, and A. Lamb, "Application of an optical remote sensing model," In: *Proc. European Optical Society and SPIE - The International Society for Optical Engineering (EUROPTO), The European Symposium on Satellite Remote Sensing*, Paris, France, 25-28 September, 1995, Volume 2586, pp. 32-43.

6. A. Lamb, Sensitivity analysis of an optical remote sensing model, Master Thesis, Florida Institute of Technology, 1995, 136. pp.

7. G. Suits, "The calculation of the directional reflectance of a vegetative canopy," *Remote Sens. Env.*, 1972, 2, 117.

8. A. Schuster, "Radiation through a foggy atmosphere," *Astrophys. J.*, 21(1), 1905, 1-22.

9. R. Priesendorfer, Hydrologic Optics, Vol I-VI, NOAA/ERL, Honolulu, HI, 1976, 1757 pp.

10. S. Ackleson, A two-flow model to simulate the interaction of irradiance with a submerged plant canopy, Ph.D. Dissertation, University of Delaware, 1985, 139 pp.

11. S. Valley, "Handbook of geophysics and space environments," Air Force Cambridge Research Laboratories, 1.0-22.15 (1965).

12. L. Elterman, "Vertical-attenuation model with eight surface meteorological ranges 2 to 13 kilometers" AFCRL-70-0200, 1970, 57 pp.

13. "On the nature and Distribution of Solar Radiation," U.S. Dept. of Energy, HCP/T2552-01, (1978)

14. R. Bukata, J.E. Bruton, and J. Jerome, "Use of chromaticity in remote sensing measurements of water quality," *Remote Sen. Env.*, 13, 1983, pp. 161-177.

15. R. Smith and K. Baker, "Optical properties of the clearest natural waters, *Appl. Opt.*, 20(2), 1981, pp. 177-184.

16. C. Bostater and M. Gimond, "Using aircraft based high resolution reflectance signatures and specific absorption coefficients to remotely estimate coastal water quality," In: *Proc. 2nd Intl. Airborne Remote Sensing Conference and Exhibition*, San Francisco, CA, 24-27 June, 1996, pp. 635-645.

17. C Bostater and M. Gimond, "Methodology evaluation for remotely estimating water quality parameters in estuarine waters," In: *Proc. European Optical society and SPIE - The International Society for Optical Engineering (EUROPTO), The European Symposium on Satellite Remote Sensing II*, Paris, France, 25-28 September, 1995, volume 2586, pp. 14-25.

18. H. Gordon, Modeling and Simulating Radiative Transfer in the Ocean, In: Ocean Optics, ed. R. W. Spinrad, K. L. Carder, and M. J. Perry, Oxford University Press, New York, NY, 1994, 283 pp.

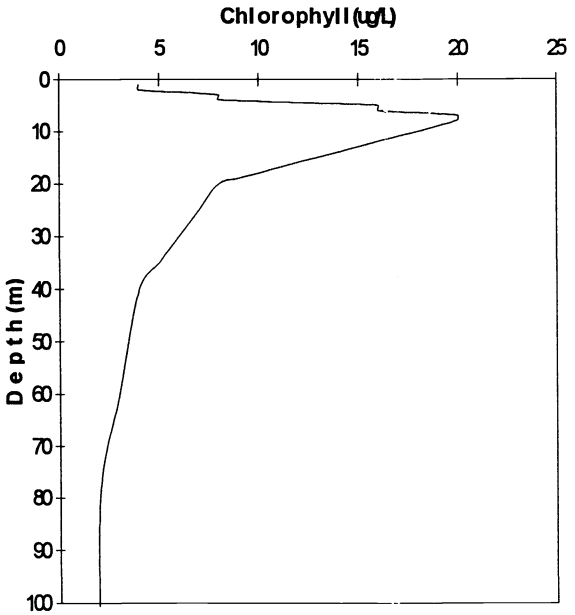

Figure 1. Vertical distribution of chlorophyll used in the model runs. The concentration is constant (2μg/L) below 80 m down to the bottom.

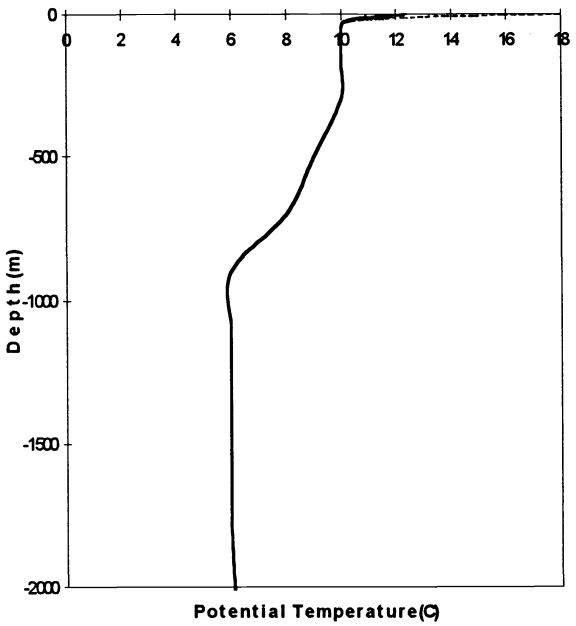

Figure 2. Vertical temperature profile after 30 days. Dotted line is the two-flow model, solid line is exponential attenuation. Note the seasonal thermocline at the top as well as the permanent thermocline from 500 to 1000 m.

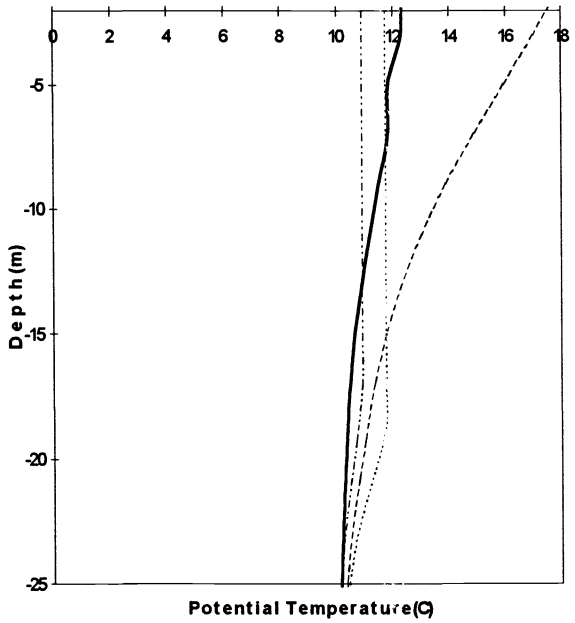

Figure 3. Vertical temperature profile from Figure 2, showing the first 25 m. Dotted lines are profiles after 10, 20, and 30 days when two-flow irradiance transfer is used, and the solid line is the profile generated after 30 days when Jerlov's coefficients are used. This run used coefficients for pure sea water.

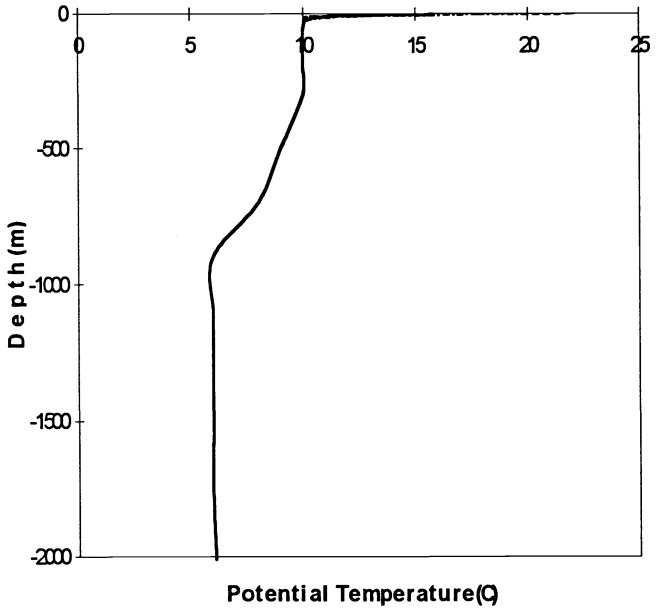

Figure 4. Vertical temperature profile after 30 days. Dotted line used the two-flow model for irradiance transfer, and the solid line is exponential attenuation. This run used coefficients for more turbid water (10 mg/L seston).

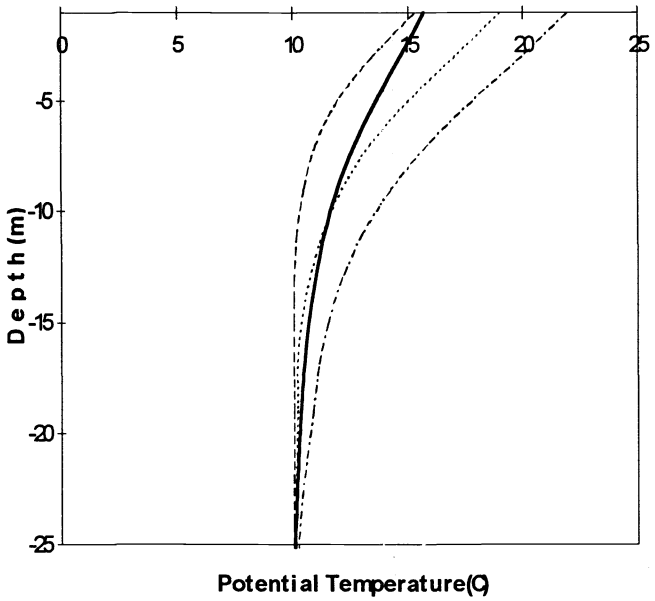

Figure 5. Vertical temperature profile from Figure 4 showing the first 25 m. Dotted lines are profiles after 10, 20 and 30 days when two-flow irradiance transfer is used, and the solid line is the profile generated after 30 days using exponential attenuation. Note the higher surface temperature when compared with Figure 3 for clear water.

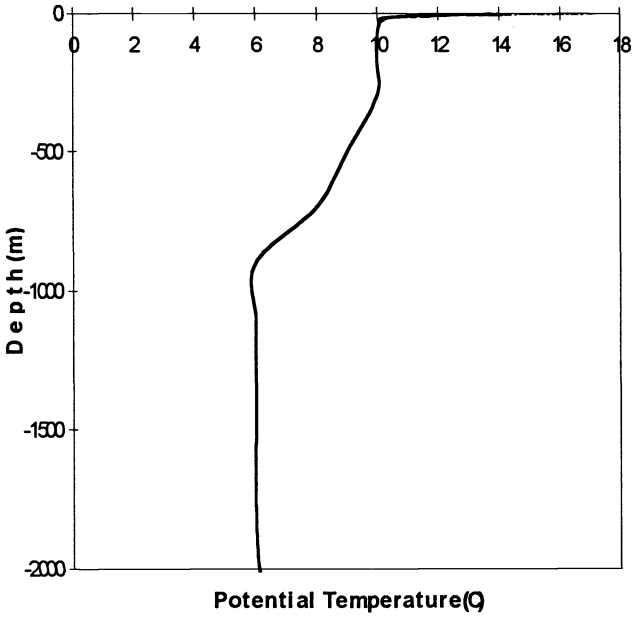

Figure 6. Vertical temperature profile after 30 days. Dotted line used the two-flow model for irradiance transfer, and the solid line is exponential attenuation. This run used the vertical distribution of chlorophyll given in Figure 1.

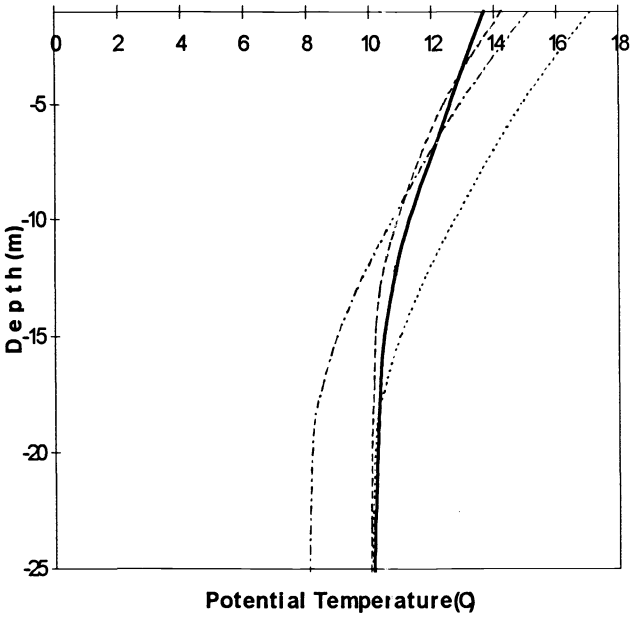

Figure 7. Vertical temperature profile from Figure 6 showing the first 25 m. Dotted lines are profiles after 10, 20 and 30 days when two-flow irradiance transfer is used, and the solid line is the profile generated after 30 days using exponential attenuation.

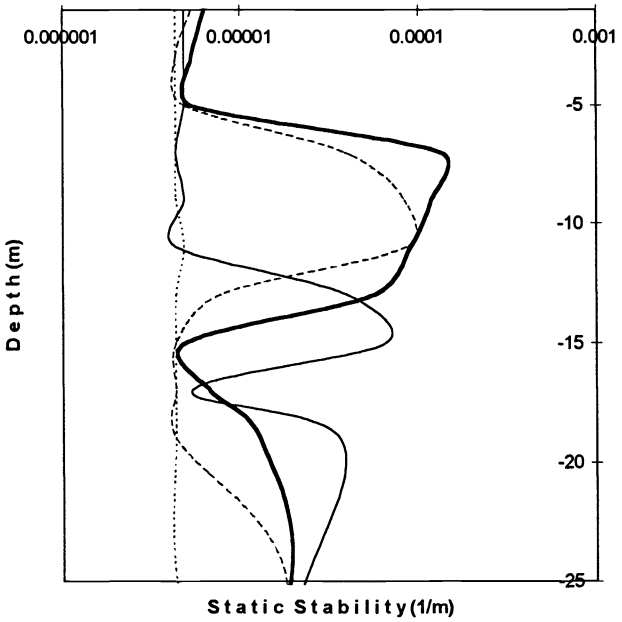

Figure 8. Static stability after 30 days for three different water masses using two-flow attenuation (bold line is constant 10 mg/L seston, solid line is water with the chlorophyll concentration from Figure 1, and dashed line is clear water) and Type I water (dotted line) using exponential notation.

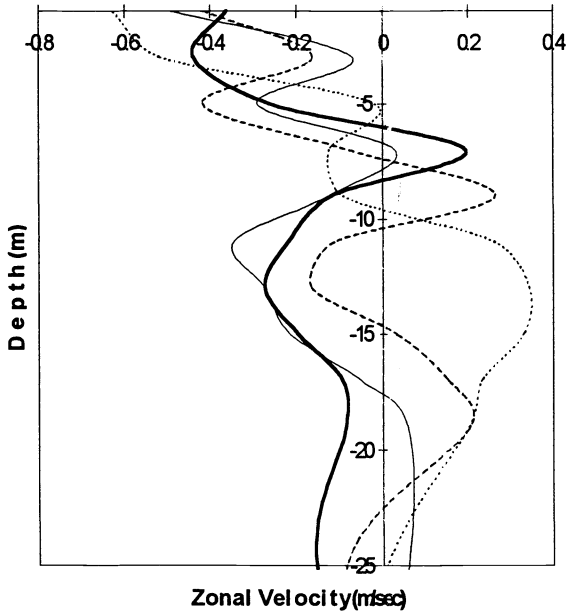

Figure 9. Zonal (u) velocity after 30 days for the same water masses and attenuations from Figure 8.

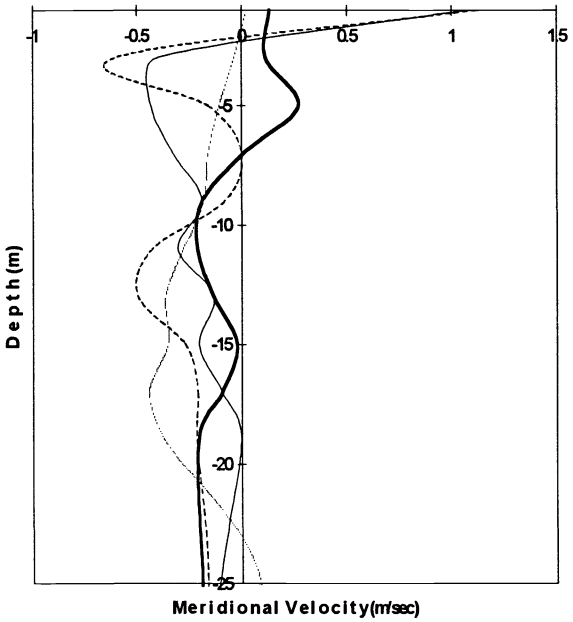

Figure 10. Meridional (v) velocity after 30 days for the same water masses and attenuations from Figure 8.

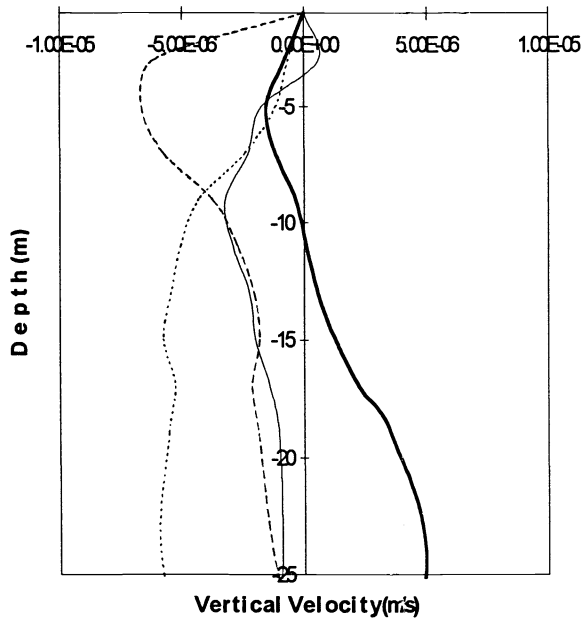

Figure 11. Vertical velocity after 30 days for the same water masses and attenuations from Figure 8.

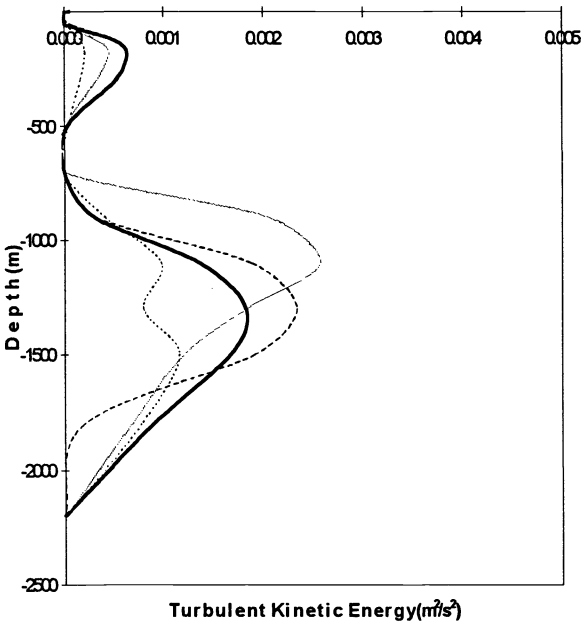

Figure 12. Turbulent kinetic energy (m^2/s^2) after 30 days for the same water masses and attenuations from Figure 8.